PERGAMON

International Journal of Impact Engineering 26 (2001) 421–431

INTERNATIONAL JOURNAL OF IMPACT ENGINEERING

www.elsevier.com/locate/ijimpeng

EFFECT OF ALIGNMENT ON THE PENETRATION OF SEGMENTED RODS

DAVID L. LITTLEFIELD

The Institute for Advanced Technology, The University of Texas at Austin,
3925 W. Braker Ln., Ste. 400, Austin, TX 78759, USA

Abstract—The purpose of this investigation is to study the effect of alignment on the performance of segmented penetrators. The Eulerian wave propagation code CTH is used for this purpose. A series of calculations using four L/D = 1 tungsten alloy segment trains at varying degrees of misalignment is performed, impacting a single finite-thickness oblique armor steel plate. Obliquity angles of 30° and 60° were considered. This study was performed primarily to investigate the effects of obliquity and is a continuation of a previous study [1] where semi-infinite armor steel plates were examined. It is shown that the obliquity of the plate can have a significant influence on the performance of the segment train. When misalignment is minimal, the performance of the segment train is not adversely affected, particularly if the misalignment positions the train in an orientation aligned with the plate normal. However, for large misalignments, degradation to the performance of the segment train is significant at all orientations.

INTRODUCTION

It is well known that the penetration depth P of cylindrical penetrators, when normalized by the length L, increases as the aspect ratio L/D decreases. This is particularly true of $L/D < 1$ penetrators at hypervelocities. The phenomena suggests that the penetration depth of large aspect ratio penetrators can be increased if the penetrator is subdivided into a large number of short L/D segments. If the benefits can be fully achieved, there are significant performance gains to be realized for segmented penetrators; for example, the penetration efficiency P/L can be increased by a factor of two or more and does not approach a limiting value as the velocity is increased.

In practice, however, there are difficulties associated with the implementation of segmented penetrators, including launch and flight and terminal ballistic limitations. For example, it is essential that the segment train remain highly aligned during penetration; slight offsets in the alignment of subsequent segments can result in interference with the sidewalls of the penetration channel and degradation of performance. This has been examined in previous studies, where segmented rods were impacted onto semi-infinite armor steel targets [1].

A possible source of segment misalignment is associated with the deployment of a segmented penetrator. For example, one way to produce a segmented penetrator might be to launch it in a collapsed (parent) configuration and separate the segments during flight. As the parent rod flies, it is subject to a cyclic damped pitching motion that is a natural consequence of launching long rods. Thus, when the segments are deployed it is likely that the segment train will have pitch associated with it, as is shown in Fig. 1. Naturally, the cyclic pitching must stop after the segments are deployed since it is elastic bending down the length of the rod that causes the pitching motion. After separation, the center-to-center offset of the segments, δ, is related to the

0734-743X/01/$ - see front matter
PII: S0734-743X(01)00092-6

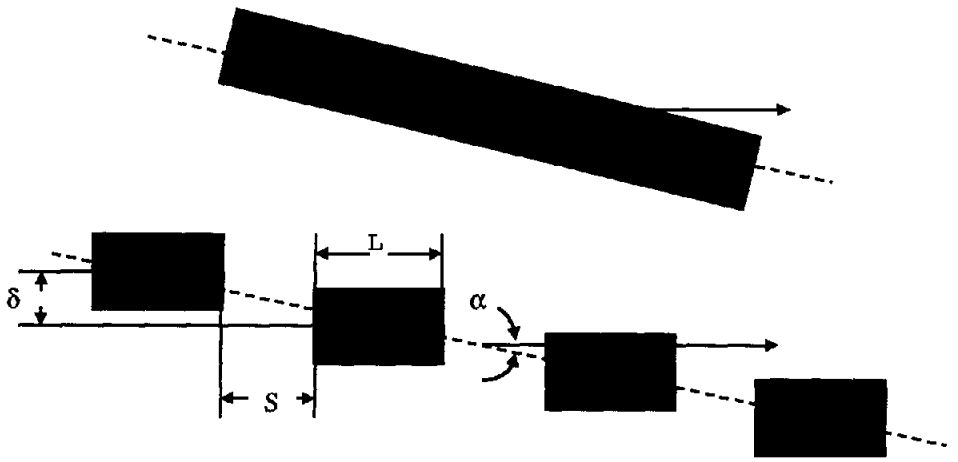

Fig. 1. Deployment of a segment train.

segment geometry and the pitch α of the parent rod at the time of deployment as $\delta = (S + L) \tan \alpha$.

To assess the performance of segmented rods, it is important to consider realistic target geometries. Real targets contain materials and geometries other than semi-infinite armor steel considered in the previous study [1], and the details of the target configuration will most likely impact on the performance of the segmented rod. To begin addressing this problem, a numerical study was conducted to examine the performance of segmented rods against finite thickness, oblique plates. The eulerian hydrocode CTH is used for this purpose. It is demonstrated that alignment of the segments can have a considerable impact on the performance of the penetrator. This is particularly true when the segments are aligned in their most unfavorable direction relative to the plate.

SETUP FOR CALCULATIONS

Numerical simulations were carried out using the three-dimensional, multi-material Eulerian hydrocode CTH [2]. CTH uses the van Leer algorithm for second-order advection that has been generalized to account for a non-uniform and finite grid, and multiple materials; CTH also has an advanced material interface algorithm for the treatment of mixed cells [3]. Several advanced equation-of-state and constitutive models are available in the code [4].

The target and penetrator geometry used in the simulations is presented in Figure 2. The target plate has a length l of 600 mm and a width w of 250 mm. The large lateral dimensions were necessary to preclude edge effects for situations involving very large misalignments. Target obliquity angles θ of 30° and 60° were considered. The thickness t of the plates was set to 80.0 and 46.2 mm for the 30° and 60° oblique plates, respectively, so that the line-of-sight thicknesses were the same. The segments are 12 mm in diameter with $L/D = 1$. The segment spacing S was kept at 30 mm so that $S/D = 2.5$, and the impact velocity V was set to 3 km/s. Four segments were used in each simulation. Symmetry of the impact scenario at $z = 0$ was exploited; in the simulations and only half of the problem was run (refer to Fig. 2 for the location of the z - axis). A total of eight zones were used across the diameter of the penetrator. The zoning was maintained cubical in regions of the grid where strong interactions were expected, estimated to be one penetrator diameter beyond furthest lateral extent of the target hole and penetrator, and through the entire thickness of the plate along the shotline (complete perforation

was expected for the aligned case). A zoning sensitivity study was not performed, but previous studies for long rods have shown that this zoning is adequate to provide reasonable numerical convergence [5].

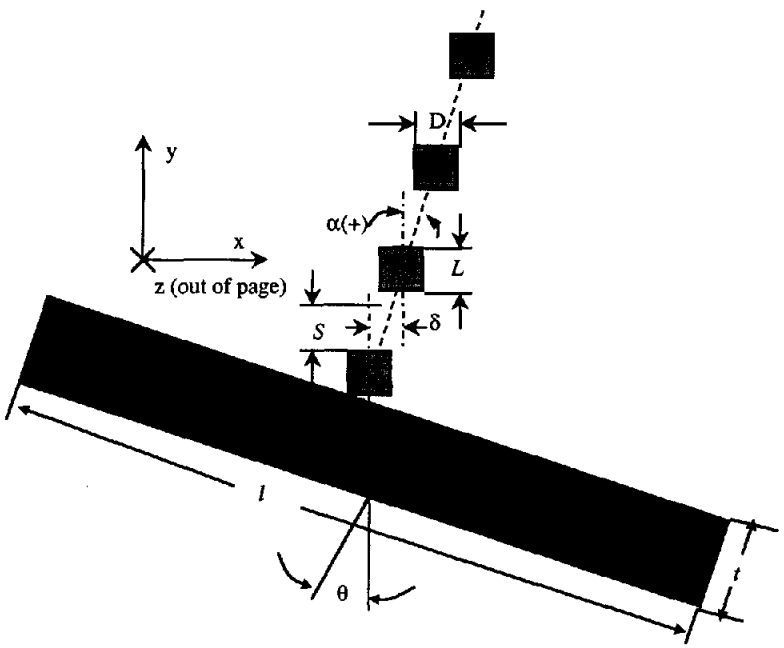

Fig. 2. Setup for computations.

In Table 1, specifics of the geometry variations considered in each of the computations are described. These calculations were performed for obliquity angles of 30 and 60 degrees, so a total of 22 calculations were conducted. The equivalent pitch angle α is also given for each condition. Positive pitch angles denote misalignments resulting in orientations more aligned with the plate normal (see Figure 2), and negative values in the opposite direction. Note that the pitch angles listed are quite large in magnitude compared to the value that might be anticipated from the deployment of a segment train. However, longer segment trains at more realistic pitch angles will still result in channel sidewall interactions during the later stages of penetration; the short segment trains considered here simply start their interactions earlier, and can be run with considerably less computer time.

Table 1. Segment train dimensions (target obliquities of 30° and 60° were considered)

δ (MM)	0	3.0	6.0	12	18	24	3.0	6.0	12	18	24
δ/D	0	0.25	0.5	1.0	1.5	2.0	0.25	0.50	1.0	1.5	2.0
α (deg)	0	4.1	8.1	15.9	23.2	29.7	-4.1	-8.1	-15.9	-23.2	-29.7

RESULTS

Results from the simulations of the four-segment train are summarized in Figure 3, where two measures of penetration efficiency (the penetration depth, normalized by both L and nL, where n is the number of segments), are shown versus the normalized offset δ/D. For comparison, comparable values for semi-infinite targets given in [1] are also given. The values for P extracted from the simulations are the deepest points of penetration measured along a direction parallel to the original line-of-sight. For small δ, the deepest point of penetration generally coincides with the line-of-sight direction, but at larger offsets deflection of the segments changes the location of maximum penetration. In about half the cases simulated, the segment train perforated the plate, and in these cases the residual penetration was estimated, based on the length and velocity of the residual penetrator, and was added onto the line-of-sight penetration.

The results in Figure 3 show that when $\delta = 0$ (i.e. the segment train is aligned), the value for P/nL approaches a limit close to its value for a $L/D = 1$ cylindrical penetrator, which is about 2.2 at this velocity (see, for example, Ref. [6]). As such, for this spacing, interference between the segments is minimal and the total penetration depth is about equal to the sum of the penetration depths for each of the individual segments. Likewise, Figure 3 shows that when δ/D is larger than two, P/L approaches its limiting value for an $L/D = 1$ segment, indicating that at this offset each of the projectiles in the segment train penetrate the target in an independent manner. The limiting value for 60° obliquity is slightly larger than the value at 30° obliquity, due primarily to the fact that the deepest point of penetration is no longer coincident with the line-of-sight. There is a slight increase in penetration efficiency that occurs when $\delta = 0.25D$ for negative and $0.50D$ for positive pitch angles, which is probably somewhat anomalous since it is caused by an elongation of the fourth segment in the train. As was pointed out in previous work [1], this elongation is not physical and is an artifact caused by the simple fracture model used in the simulations.

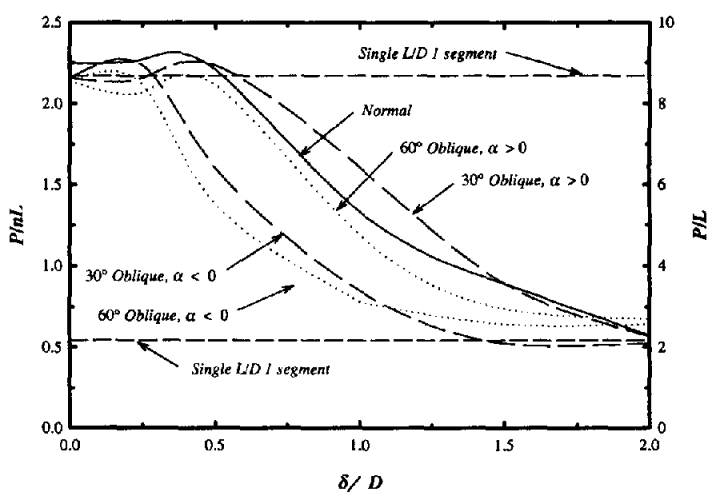

Fig. 3. Penetration efficiency versus normalized offset for impact of a four-segment train on an oblique target.

For intermediate values of δ, it is clear from Figure 3 that the target obliquity and orientation of the alignment plays an important role in determining the performance of the segment train. For the 30° target with positive pitch angles at offsets less than about a diameter, the degradation in performance is somewhat delayed compared to a normal impact at the same pitch. This is not a surprising result since positive pitch angles tend to align the segment train with the normal to the plate. However, for offsets above a diameter, this advantage rapidly diminishes and the performance of the segment train is very similar to the result obtained for the normal impact situation. Similar behavior is seen for the 60° target for positive pitch angles. On the other hand, for negative pitch angles the performance of the segment train rapidly diminishes even at offsets below $0.5D$. Degradation in performance also tends to increase with obliquity, except at large offsets, which is due primarily to the deepest point in penetration no longer coinciding with the line-of-sight.

Details of the penetration behavior are illustrated in Figs. 4 – 13, where material plots are shown at various times for offsets of 0, $0.5D$ and $1.0D$, for the two obliquity angles at both positive and negative pitch angles. When the offset is zero, Figs. 4 and 5 show that the segment train penetrates with no interference from the sidewalls of the cavity, albeit the clearance on the upward facing surface of the crater is very slight. It is also evident that nearly complete erosion of segments has occurred at the time of arrival of subsequent segments at the base of the crater, suggesting that the performance of the segment train in this case is nearly optimal and equal to n times the penetration of a single segment (this was also seen in Figure 3). The fourth segment perforates the plate with a residual segment of $L/D \approx 1/5$ remaining for each of the targets. In Figs. 6 and 7, material plots are shown for $\delta = 0.5D$ and negative pitch for targets at 30° and 60° obliquity, respectively. At this offset, the segment train immediately interferes with the sidewall of the crater; a result of the asymmetry in the crater and the reduced clearance on the upward side of the cavity. At 20 μs, Fig. 6a shows that the second segment is somewhat elongated and deflected from its interaction with the sidewall, this interaction is more pronounced in Fig. 7a. By 40 μs the second segment strikes the base of the penetration channel; for the 30° target the change in penetration caused by this segment is actually a little larger than the value observed for $\delta = 0$ because of the elongation, but for the 60° target it is less. The third segment has also entered the penetration channel and is significantly elongated and deflected by the crater sidewall. At 100 μs, Fig. 6d shows that the fourth segment has perforated the plate with no residual length; there is no perforation in Fig. 7d for the 60° target. The final penetration cavities for these two targets exhibit different penetration paths as a result of the sidewall interaction. The 30° target exhibits a path that is somewhat aligned with the direction of the original orientation in the segment train, but the path for the 60° target is much larger in lateral extent, indicating that the impact of subsequent segments does very little to increase penetration.

In Figs. 8 and 9, on the other hand, where results for positive pitch are shown for $\delta = 0.5D$, there is very little evidence of interference between segments and the cavity sidewall. For the 30° target, only the fourth segment interferes with the sidewall; there is no interaction for the 60 ° target. The interference results in an increase of effective length for the fourth segment, which actually improves the overall performance of the segment train, but as was discussed previously, this improvement is probably anomalous. As the offset is increased further, more substantial degradation in the performance occurs. Shown in Figs. 10 and 11 are material plots for the two targets at various times for $\delta = 1.0D$ and negative pitch. It is evident from this sequence that each of the segments penetrates almost independently; subsequent segments do not impact the base of the original penetration channel. This is particularly true of the 60° target. This was also clearly illustrated in Figure 3, where the penetration efficiency for $\delta = 1.0D$ and negative pitch is nearly equal to its limiting value for a single segment. However, when the pitch angle is positive this process is delayed, as is illustrated in Figs. 12 and 13, where material plots for the two targets are given for $\delta = 1.0D$ and positive pitch. Here, the second segment does not

interact with the sidewall and strikes the base of the original crater created by the first segment. For the 30° target, the third segment is elongated from sidewall interaction and actually penetrates the deepest of all four segments; the fourth segment does not reach the base of the crater. The fact that plate perforation occurs in this case clearly is a misleading interpretation of the performance, since the penetration path was the actually shortened by the offset, and the final geometry of the crater will not permit additional segments to pass through without significant interaction. All the segments for the 60° target, on the other hand, penetrate relatively independently at this offset.

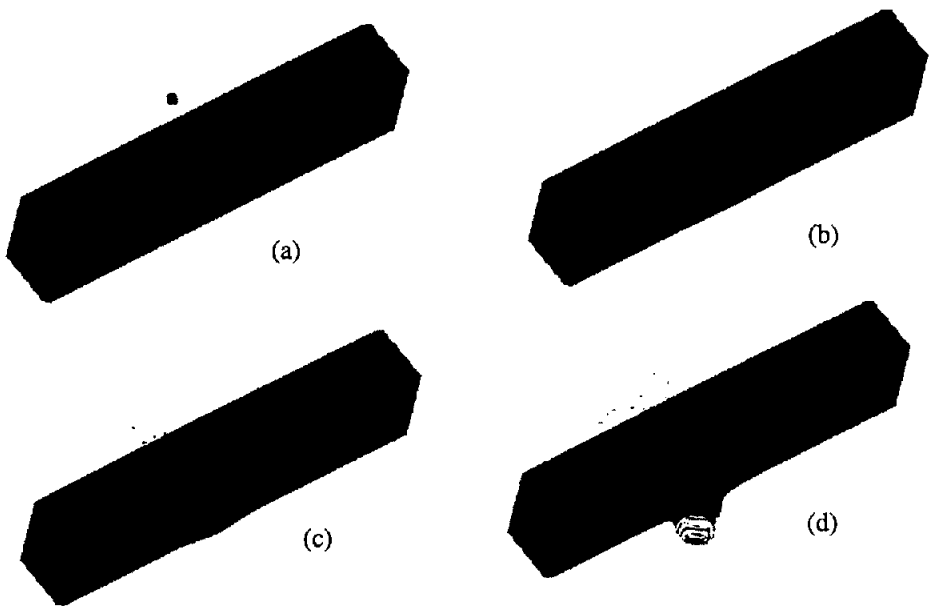

Fig. 4. Penetration channel geometry from the impact of a four L/D = 1 segment train on a 30° oblique plate with δ/D = 0 at various times after impact: (a) 15 μs, (b) 40 μs, (c) 60μs, and (d) 100 μs.

Fig. 5. Penetration channel geometry from the impact of a four L/D = 1 segment train on a 60° oblique plate with δ/D = 0 at various times after impact: (a) 15 μs, (b) 40 μs, (c) 60μs, and (d) 100 μs.

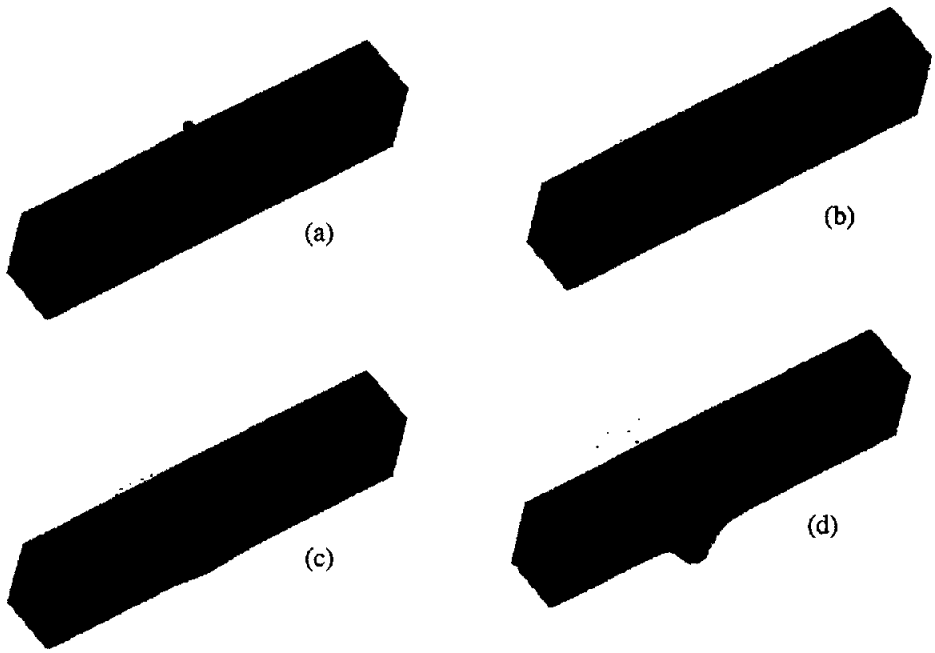

Fig. 6. Penetration channel geometry from the impact of a four $L/D = 1$ segment train on a 30° oblique plate with $\delta/D = 0.5$ and $\alpha < 0$ at various times after impact: (a) 20 μs, (b) 40 μs, (c) 60μs, and (d) 110 μs.

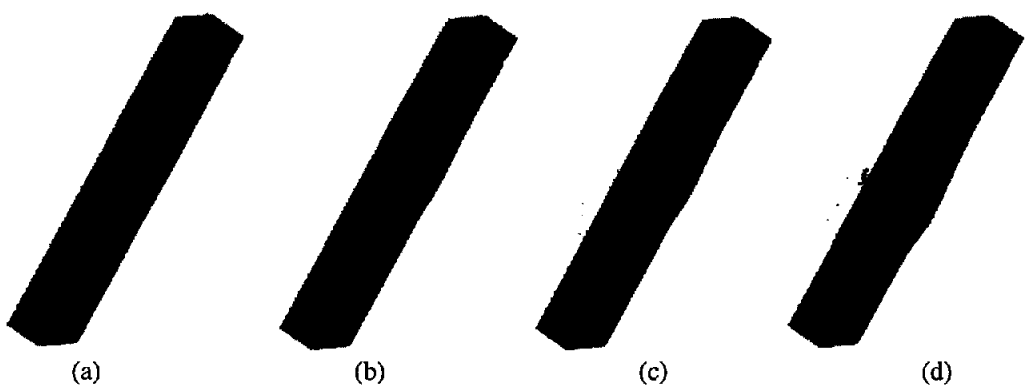

Fig. 7. Penetration channel geometry from the impact of a four $L/D = 1$ segment train on a 60° oblique plate with $\delta/D = 0.5$ and $\alpha < 0$ at various times after impact: (a) 20 μs, (b) 40 μs, (c) 60μs, and (d) 110 μs.

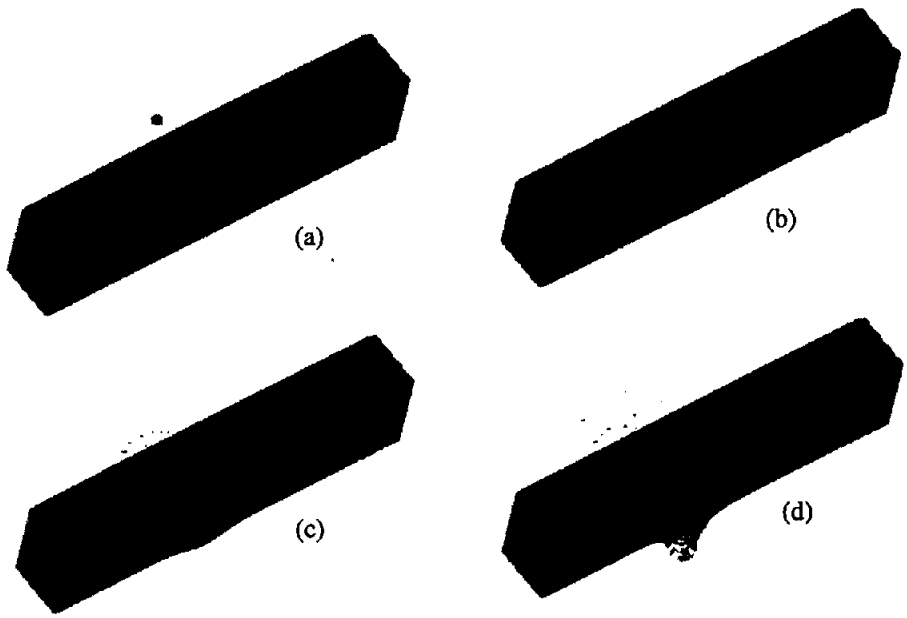

Fig. 8. Penetration channel geometry from the impact of a four $L/D = 1$ segment train on a 30° oblique plate with $\delta/D = 0.5$ and $\alpha > 0$ at various times after impact: (a) 20 μs, (b) 40 μs, (c) 70μs, and (d) 100 μs.

Fig. 9. Penetration channel geometry from the impact of a four $L/D = 1$ segment train on a 60° oblique plate with $\delta/D = 0.5$ and $\alpha > 0$ at various times after impact: (a) 20 μs, (b) 40 μs, (c) 65μs, and (d) 140 μs.

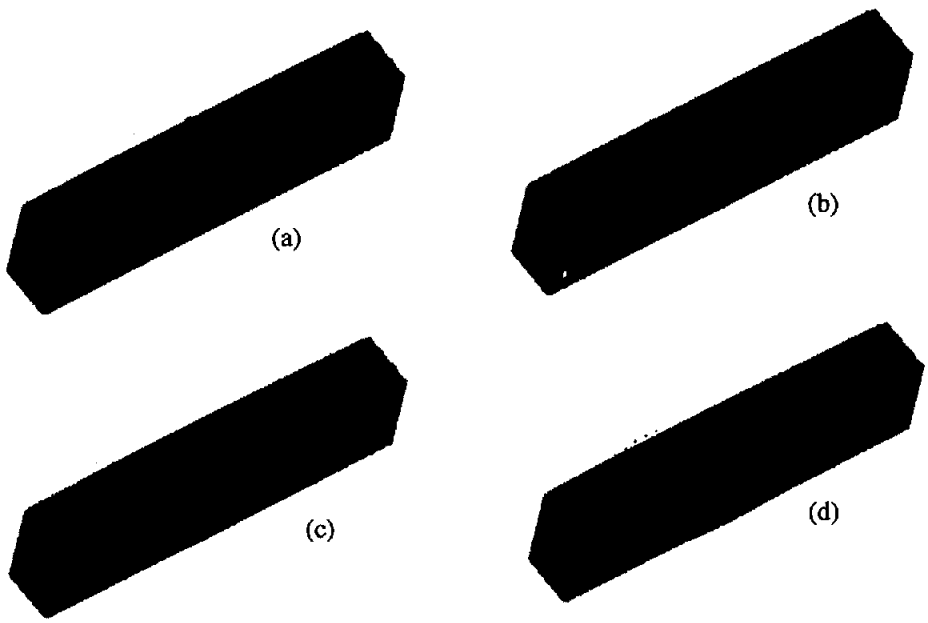

Fig. 10. Penetration channel geometry from the impact of a four L/D = 1 segment train on a 30° oblique plate with δ/D = 1.0 and $\alpha < 0$ at various times after impact: (a) 15 μs, (b) 30 μs, (c) 40μs, and (d) 70 μs.

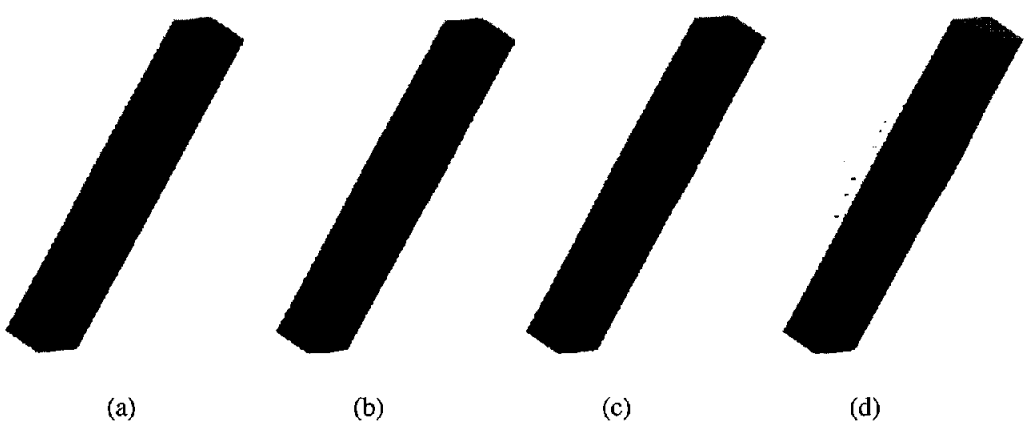

Fig. 11. Penetration channel geometry from the impact of a four L/D = 1 segment train on a 60° oblique plate with δ/D = 1.0 and $\alpha < 0$ at various times after impact: (a) 15 μs, (b) 30 μs, (c) 40μs, and (d) 70 μs.

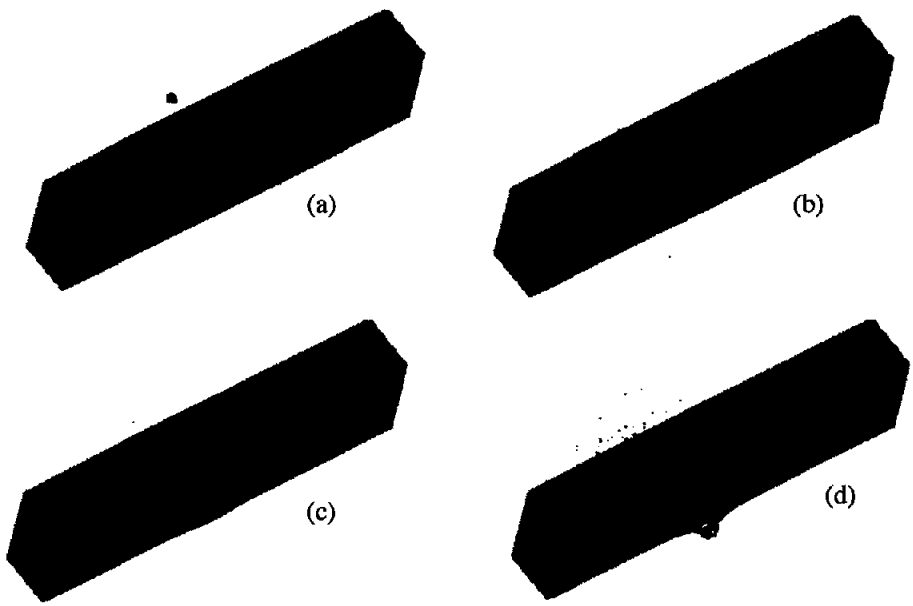

Fig. 12. Penetration channel geometry from the impact of a four $L/D = 1$ segment train on a 30° oblique plate with $\delta/D = 1.0$ and $\alpha > 0$ at various times after impact: (a) 20 μs, (b) 40 μs, (c) 60μs, and (d) 110 μs.

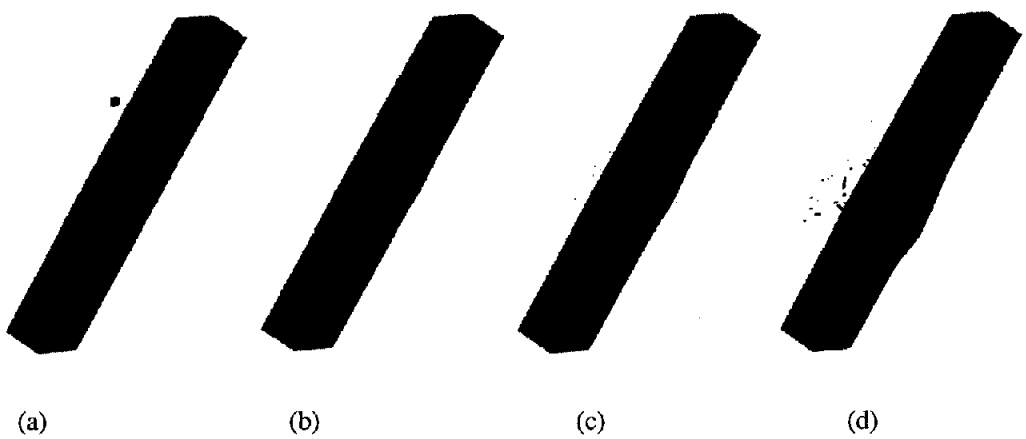

Fig. 13. Penetration channel geometry from the impact of a four $L/D = 1$ segment train on a 60° oblique plate with $\delta/D = 1.0$ and $\alpha > 0$ at various times after impact: (a) 20 μs, (b) 40 μs, (c) 60μs, and (d) 110 μs.

CONCLUSIONS

The effect of alignment on the performance of segmented penetrators was investigated in this study. The results show that when the offset is enough to produce interference between the trailing segments and the sidewall of the penetration cavity, the degradation in penetration can be significant. The obliquity of the plate can also have a significant effect on the performance of the segment train.

Acknowledgement—This work was supported by the U.S. Army Research Laboratory (ARL) under contract DAAA21-93-C-0101. The help of Mrs. Rick Garcia and David Fuentes, who performed most of the computations, is greatly appreciated. Computational resources were provided by the Texas Advanced Computation Center at the University of Texas at Austin.

REFERENCES

[1] Littlefield DL, Garcia RM, Bless S J. The effect of offset on the performance of segmented penetrators. *Int. J. Impact Engng.*, to appear.

[2] McGlaun JM, Thompson SL, Elrick MG. CTH: A three dimensional shock wave physics code. *Int. J. Impact Engng.*, 1990; **10**: 351–360.

[3] Bell RL. An improved material interface reconstruction algorithm for eulerian codes. *Sandia National Laboratories Report*, Sept. 1992; No. SAND 92-1716.

[4] Silling SA. Stability and accuracy of differencing methods for viscoplastic models in wavecodes. *J. Comp. Phys., 1993;* **104**(1): 30–40.

[5] Littlefield DL, Anderson Jr. CE. A study of zoning requirements for 2-D and 3-D long-rod penetration. *Proc. 1995 APS Topical Conference on Shock Compression of Condensed Matter*, Seattle, WA, 1995.

[6] Anderson CE, Morris BL, Littlefield DL. A penetration mechanics database. *SwRI Report No. 3593/001*, Jan. 1992.